


Manbodh Kumar Mishra <sup>1</sup>, V. P. Chandramohan <sup>1</sup>,  
Karthik Balasubramanian<sup>1</sup>

## Comparative study of cooling of automobile LED headlights without and with fins and finding comfortable operating conditions

LED light must be cooled to avoid reaching a certain temperature. Two different 3D practical domains of LED light are modelled, (i) square aluminium plate with a cylindrical plate and an LED module (model I), (ii) the same provision of model I with 25 fins (model II). ANSYS 16.0 is used for solving the problem. Temperature distribution, junction temperature ( $T_j$ ) and heat flux are estimated. Analyses are carried out for various ambient temperatures ( $T_a$ ) and for different LED power dissipations ( $Q$ ) to identify the safe operating conditions. In model I, it is found that 38% of working conditions go beyond the critical limit of  $T_j$  and it is reduced to 21.4% in model II. In model II, for low  $T_a$  of 30 and 40°C with all  $Q$  considered in this analysis are safer. If  $T_a$  is between 30 and 80°C, then  $Q$  must be maintained at 0.5 to 1.25 W. Beyond this, conditions are not safe.

### Nomenclature

$c$	constant
$D$	diameter of fin (m)
FEM	finite element method
$h$	heat transfer coefficient ( $\text{W}/\text{m}^2\text{K}$ )
$k$	thermal conductivity ( $\text{W}/\text{mK}$ )
$L$	length of fin (m)
LED	light emitting diode
$m$	slope

✉ V.P. Chandramohan, e-mail: [vpcm80@nitw.ac.in](mailto:vpcm80@nitw.ac.in)

<sup>1</sup>Department of Mechanical Engineering, National Institute of Technology Warangal, Telangana, India



© 2019. The Author(s). This is an open-access article distributed under the terms of the Creative Commons Attribution-NonCommercial-NoDerivatives License (CC BY-NC-ND 4.0, <https://creativecommons.org/licenses/by-nc-nd/4.0/>), which permits use, distribution, and reproduction in any medium, provided that the Article is properly cited, the use is non-commercial, and no modifications or adaptations are made.

MCPCB	metal-core printed circuit board
PCB	printed circuit board
$Q$	heat flow (W)
$S$	distance between the fins (m)
$T$	temperature ( $^{\circ}\text{C}$ )
$x, y, z$	coordinates

### Subscripts

$a$	ambient
$j$	junction
$s$	surface

## 1. Introduction

One cannot forget the ancient transportation system such as vehicles' wheel with 50 pieces, light weight chariots, wheels lubricated with animal fats etc. Such an automotive field achieves lot of improvisation in recent days such as alloy wheels, light emitting diode (LED) headlight, automatic gear system, power braking system and advanced suspension system [1]. Invention of LED is a historical movement in electronics field and its use in automobile sector is unavoidable. It is fitted in a vehicle's front and rear sides and sometimes on top of the vehicles. It lights the road so the driver can drive the vehicle with more visibility. Also, it is used for other drivers and pedestrians to identify the presence, distance, size and direction of vehicles. Sometimes, a driver's intention of overtaking, speeding and turning left or right are signalled by these LED lights. LED does not emit ultraviolet or infrared wavelengths, is efficient compared to other light sources and has superior longevity. One advantage of LED light is its long service life of 100,000 hours depending on use. However, the efficiency and life are degraded greatly when it is operated at a higher ambient temperature (air temperature surrounded by LED light,  $T_a$ ). Since LEDs convert 75–85% of input electric power into heat, increasing the input power can drastically increase the junction temperature ( $T_j$ ) of the LED, which is the highest operating temperature of the surface where LED headlamp is fitted.

The resulting increase in temperature affects the longevity of LED and if  $T_j$  exceeds the maximum operating temperature ( $125^{\circ}\text{C}$ ), then LEDs may lead to high thermal risks such as failures in printed circuit board (PCB), reduction in light output, significant decrease in life and finally, melting of electrical wires, therefore an electrical short circuit and thereby chances of fire accidents. The most important parameter for LEDs is  $T_j$ , which directly affects the life, lighting power and photometric value of LED. Therefore, it must be estimated and analysed for different power inputs. Addition of fins is required if comfortable  $T_j$  cannot be achieved.

There are many studies on cooling of LED headlights of automobile vehicles. Experimental and numerical analyses were performed for a pin-fin type LED

automobile headlamp by X-J Zhao et al. [2]. Effect of  $T_a$ ,  $T_j$ , heating power and tilt angle of LED light were analysed. Uncertainty analysis was performed to identify the accuracy of experimental results. They found that the  $T_j$  linearly varies with  $T_a$ .

Jang et al. [3] analysed different orientations of cylindrical heat sinks to cool an LED light. In this study, the effect of angle of inclination on heat sink was studied. It was mentioned that orientation  $0^\circ$  gave best heat transfer performance, because air flow was upward and hence all fins were vertically placed. When the angle of inclination was  $45^\circ$ , inflow air was first obstructed by the fins and then raised. This blocking effect was increased with an increased angle of inclination and hence flow velocity was decreased. When the angle of inclination was  $90^\circ$ , flow separation occurred to the left and right side of LED bulb due to the fins existing on the lower part of the heat sink.

An experimental analysis was carried out to estimate the lifetime of automobile headlights by Wang et al. [4]. Both laboratory and field experiments were conducted to achieve this task. Illumination spectrum distribution data was used as input data of numerical analysis to estimate the life of LED lights. They reported that the experimental and numerical data matched successfully. Sun et al. [5] presented a procedure for predicting the peak temperature ( $T_j$ ) of a heat sink using the concept of effective heat conductivity. The effective conductivity was estimated by experiments and it was compared with numerical predictions. Correlations were developed from their experimental results. A simple in appearance and easy to manufacturing double lens was developed for two-wheeler LED headlight by Luo et al. [6]. Their ultimate aim was to develop a headlight which should meet the criteria of "ECE regulation R 113 division 2" [6].

Kim et al. [7] reported thermal characterization of high power LED arrays. A heat pipe was used to transfer the heat.  $T_j$  and thermal resistance were estimated on LED arrays. It was found that the junction temperatures were  $87.6$  and  $63.3^\circ\text{C}$  for the system with and without heat pump, respectively. The measured thermal resistances of the above cases were  $1.8$  and  $2.71$  K/W, respectively. A thermo-electric cooler (TEC) was used to diffuse the heat transfer from LEDs by Lu et al. [8]. In their experimental work,  $6 \times 3$  W LEDs in two rows were used to compose the light source module. Environment temperature ( $T_a$ ) was maintained at  $17^\circ\text{C}$ . The temperatures of heat dissipation substrate of LEDs and cooling fins of a radiator were measured by K type thermocouples to evaluate the cooling performance. They found that the temperature of the substrate was only  $9^\circ\text{C}$  when an optimized TEC was used. The effect of humidity on LED light and its lenses was analysed by Kim et al. [9]. An experimental setup was developed with a glass covered LED light. There were two methods (by providing a heat pump and a fan) used to prevent the condensation of vapour on the LED lenses. They suggested heat pump method was good to reduce the condensation of vapour than by a fan.

A heat pipe system was used by Xiang-you et al. [10] to control the variation of  $T_j$  and cool the LED light. Temperature uniformity, thermal performance and thermal resistance were estimated using experiments at different inclination of heat

sink. The estimated thermal resistance was ranged between 0.19–0.31 K/W. Similar experimental analysis was carried out by Janicki et al. [11] and the  $T_j$  was measured by thermocouples. During the experiments, constant current was maintained to heat the LED light. Natural convection analysis was considered to estimate the  $T_j$ .

Yang et al. [12] performed heat transfer analysis of a high-brightness LED array on PCB under different configurations. They estimated the thermal performance of a high-brightness LED array on PCB. They developed a correlation between the location and interaction of LED light through experimental data. There were three different designs analysed and a better design was proposed based on the heat transfer analysis and maximum  $T_j$  of LED.

Shin and Jang [13] developed a finite volume-based numerical solution to estimate the  $T_j$  values and thermal characteristics of LED light. Experiments were conducted to estimate the  $T_j$  values at different input powers. Experimental and numerical values were compared and found reasonable agreement. Zhou et al. [14] analysed the thermal distribution of multiple LED module. They developed a numerical model using ANSYS software to estimate the temperature distribution of LED module. They also analysed the effect of thermal conductivity of metal-core printed circuit board (MCPCB) substrate on the heat dissipation of LED module in three different configurations, namely (i) vertical direction and (ii) the length-wise and (iii) width-wise. They developed a mathematical correlation to describe the vertical temperature distribution of LED module.

Yang et al. [15] estimated the thermal spreading resistance effect (TSRE) of a high power LED module. They investigated the effects of the dimensions variations and the influence of thermal conductivity of the substrate on the heat transfer characteristics of an LED module. They found that  $T_j$  of the graphite substrate was low compared to aluminium substrate. It was found that TSRE effect increased with decrease in substrate thickness. A novel technology was developed to fabricate LED lights by Liao and Tseng [16]. It was reported that using this technology,  $T_j$  further reduced to 5.1°C and enhancement of light output of 7%.

From the literature survey, there are a number of studies that contributed for cooling of electronic lights. Some of the works considered natural convection [2, 3] and some forced convection [4, 6] to solve LED light cooling problems. Constant temperature boundary conditions [7] were used to solve the heat conduction problems and very few using convective boundary conditions [5]. Finite volume method [11–14] and finite element method [9] were used to solve the governing equations. A limited number of studies estimated the junction temperatures [2, 6, 17] and thermal resistance [6] of LED lights. It was observed that if  $T_a$  inside the headlamp was sufficiently low (30–50°C), then  $T_j$  did not exceed the safety limit of 125°C [1, 18]. When  $T_a$  was more than 50°C,  $T_j$  of the higher powered LED (1.5 W, 2 W and 2.5 W) exceeded the safety limit. Very few studies analysed the effect of high powered LED lights [7, 9]. This problem can be solved using an aluminium plate behind the PCB [2]. However, when the ambient temperature inside the headlamp increased to 80°C, then  $T_j$  exceeded the safety limit. There is no study noticed, if  $T_j$

reaches beyond critical value. This study focuses on by keeping the above fact and there is a step taken to solve this problem by providing fins. Fins are surface that is extended from the practical domain to increase the rate of heat transfer to or from the environment by increasing convection heat transfer. It is an economical solution to heat transfer problems and hence this approach is used in the present LED light cooling problem. Also, through this analysis, a set of comfortable working conditions of LED is proposed.

The main objectives of this work are:

- To develop a numerical model of heat dissipating LED headlights by generating two practical domains namely, system without fin (model I) and model I with fins (model II).
- To estimate the junction temperature ( $T_j$ ) and heat flux of both models by varying ambient temperature ( $T_a$ ) and heat flow ( $Q$ ).
- To identify safe working conditions of LED lights on both models by varying ambient temperature ( $T_a$ ) and heat flow ( $Q$ ).
- To compare the results of both model I and model II and thereby find the percentage reduction of  $T_j$  values.
- To analyse the effect of different heat transfer coefficient ( $h$ ) on junction temperature with different heat flow ( $Q$ ).

## 2. Methodology

Fig. 1 shows the schematic diagram of a LED light without fins. It consists of socket, quartz glass, filaments, coating, LED module etc. Filament for driving (high beams) and filament for turnout (low beams) are the two filaments used inside the LED light. The automobile's headlight is adjusted to high beams to illuminate long distance in front of the car. They are usually used on highways and rural areas that don't have much traffic. Since high beams are so bright, they blind the incoming traffic. Low beams are used for normal driving and in the rain so that the other drivers can see the driver. High beam lights are usually used by drivers for illuminating the light for long distance and this is the reason LED module gets heated beyond a set temperature limit. Therefore, in this work, high beam is taken into consideration and based on that the practical domain is modelled. In the modelling part, quartz glass and filaments are eliminated. Because of the heated filament, the LED module gets heated. This heat is taken as heat flux of the LED module and it is given as input value to the numerical simulations.

Two practical domains of LED light are created, one without fins (model I) and the second one with fins (model II). The junction temperature, heat flux and temperature distribution are estimated, hence the safety limit can be identified and a better model can be proposed through this study. These two models are explained in further sections.

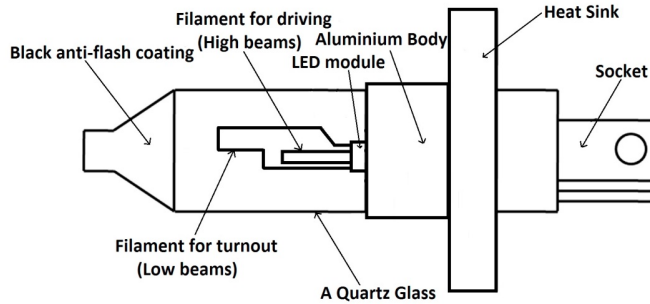


Fig. 1. Schematic of a car LED light

### 2.1. Practical domain without fin (model I)

Model I (Fig. 2) is approximately generated from Fig. 1 by removing filament part and glass portion. It makes the model simple, which is used for reducing the computational complexity without affecting the practicality of the real problem. The 2D representation of practical domain (Fig. 2) consists of an LED module, an aluminium body and heat sink. In this domain, the left cubical rectangular portion of model I (called LED module) is taken as the base surface of the filament. The amount of heat generated on the base surface of the filament is taken as the heat flow ( $Q$ ). This heat is transferred to the aluminium body, which is used to extract the heat from LED module and then to heat sink, which is also considered as aluminium material for this study. Based on that, a 3-D domain (Fig. 3) is modelled using ANSYS Design Modeler for numerical simulations. Heat sink dimensions are taken as  $40 \times 40 \times 2 \text{ mm}^3$ . The aluminium plate is cylindrical in shape with a diameter of 10 mm and length of 5 mm. The LED module dimension is  $1 \times 0.5 \times 0.5 \text{ mm}^3$ . Mesh is generated using ANSYS Multiphysics and it is shown in Fig. 4.

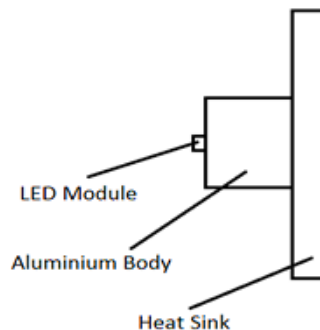


Fig. 2. 2D representation of practical domain without fin (model I)

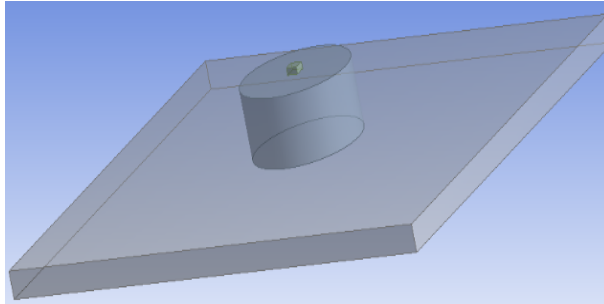


Fig. 3. 3D model of model I using ANSYS Design Modeler

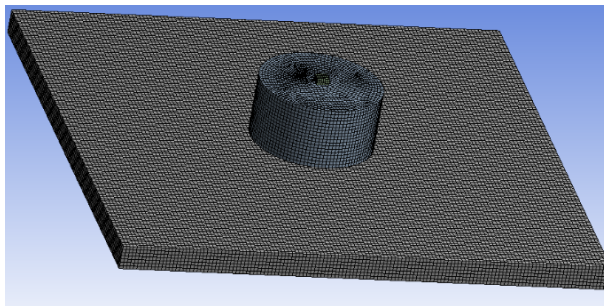


Fig. 4. Mesh generated for the model I

## 2.2. Practical domain with fin (model II)

Model II (Fig. 5) consists of the same components of model I and also has fins. Heat sink is fitted with 25 fins in  $5 \times 5$  array manner to encourage the air flow in between fins. If numbers of fins are further increased, the heat transfer may not take effectively as it affects the free air flow in the  $40 \times 40 \text{ m}^2$  heat sink surface.

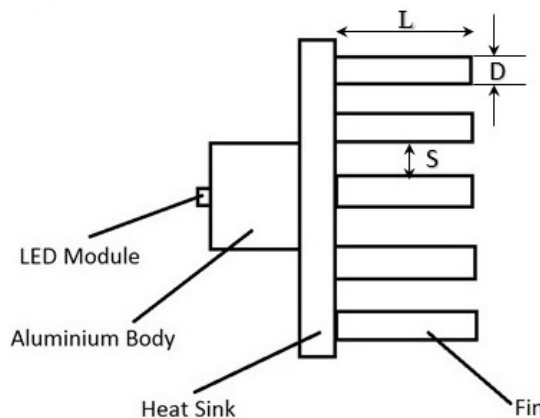


Fig. 5. 2D representation of practical domain with fins (model II)



By keeping this practicality in mind, 25 fins were selected.  $D$  is taken as diameter of fin (2 mm),  $L$  is length of the fin (10 mm) and  $S$  is the distance between two successive fins (5 mm).  $D$ ,  $L$  and  $S$  were chosen based on the space constraints of LED light and its heat sink. Based on that, a 3-D domain (Fig. 6) is modelled using ANSYS Design Modeler. Cylindrical fins (pin-fins) are used in this analysis. Mesh is generated as shown in Fig. 7.

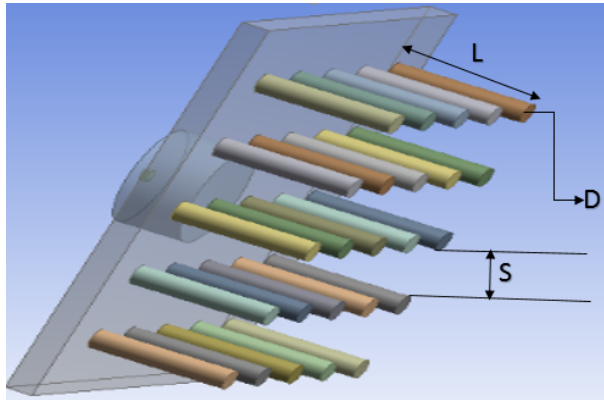


Fig. 6. 3D model generated for system with fins (model II)

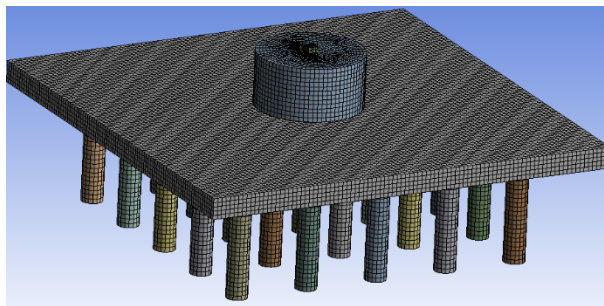


Fig. 7. Mesh generated for model II

### 2.3. Governing equations, boundary conditions and heat flux

A 3D steady-state heat conduction equation with no heat generation is represented as;

$$\frac{\partial^2 T}{\partial x^2} + \frac{\partial^2 T}{\partial y^2} + \frac{\partial^2 T}{\partial z^2} = 0, \quad (1)$$

where  $T$  is temperature to be calculated at a given point ( $^{\circ}\text{C}$ ).



Convective boundary condition (Robin boundary condition) is used to solve this problem as it is more realistic that the LED module loses heat to the air.

$$-k \frac{\partial T}{\partial x} = h(T_s - T_a) \quad (2)$$

$T_s$  and  $T_a$  are the temperatures at the surface and ambient in °C, respectively.

## 2.4. Solution procedure

ANSYS 16 (solver name: Steady-state Thermal Mechanical APDL solver) is used to run the simulations and thereby estimate the temperature distribution, junction temperature and total heat flux of LED headlamp. Free convection simulations were carried out for both models because the ambient air surrounded by LED lights has negligible air velocity as the LED lights are in an enclosure. Finite element method (FEM) is used to solve the governing equations. Newton-Raphson method is used to take the iteration process. The converging criterion for energy equation is  $10^{-6}$ .

The range of heat transfer coefficient ( $h$ ) ( $5\text{--}25 \text{ W/m}^2\text{K}$ ) was selected for free convection simulations as  $h$  varies from 5 to  $25 \text{ W/m}^2\text{K}$  for natural convection applications [19–21]. Aluminium was used as the fin material whose thermal conductivity is  $205 \text{ W/m}^2\text{K}$ . In this study, steady-state, isotropic material and laminar flow were assumed. The atmospheric pressure and ambient temperature were applied to the outer domain. The maximum temperature of the heat sink was in the range of  $100\text{--}135^\circ\text{C}$ , therefore the radiation effects are very minimal, hence the effect of radiation is not considered [15].

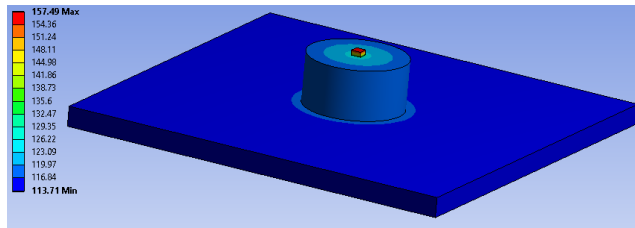
## 3. Results and discussion

In this results and discussion section, the results of model I (system without fins) and model II (system with fins) are discussed separately as follows.

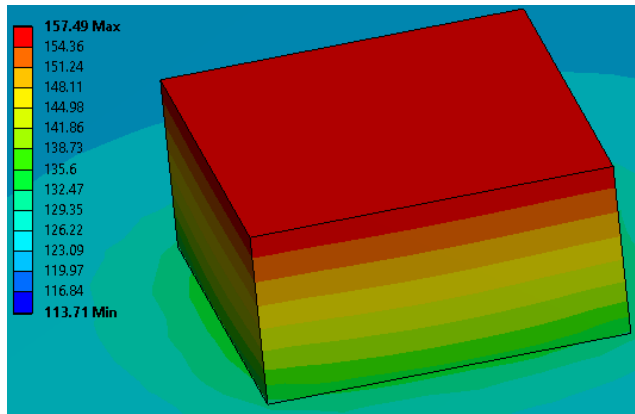
### 3.1. Results of LED system without fin (model I)

Grid independence study was performed to identify the optimum number of elements for model I.  $T_j$  was estimated at different  $T_a$  and at heat flow of  $1.5 \text{ W}$  and  $h = 10 \text{ W/m}^2\text{K}$  and it is given in Table 1. Numbers of elements were selected between 87500 to 162000. Table 1 shows the estimated  $T_j$  values at different  $T_a$  of  $30^\circ\text{C}$ ,  $40^\circ\text{C}$ ,  $50^\circ\text{C}$ ,  $60^\circ\text{C}$  and  $70^\circ\text{C}$  for elements ( $n$ ) of 87500, 112300, 137000 and 162000. At  $T_a = 30^\circ\text{C}$ , the average error of two junction temperatures between two successive elements of 137000 and 162000 is 0.0069%. Therefore, element ( $n$ ) 137000 was selected for this analysis.

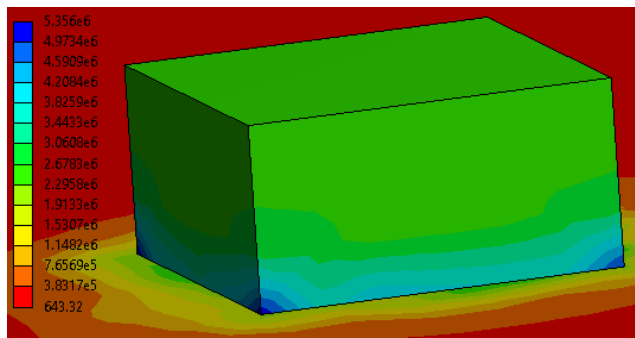
Fig. 8a shows the temperature distribution of complete domain of model I. It is plotted at  $Q = 2.5 \text{ W}$ ,  $T_a = 50^\circ\text{C}$  and  $h = 10 \text{ W/m}^2\text{K}$ . There is not much temperature



(a)



(b)



(c)

Fig. 8. (a) Complete view of temperature distribution of model I in  $^{\circ}\text{C}$ , (b) Temperature variation of top portion (LED module) in  $^{\circ}\text{C}$ , and (c) heat flux in  $\text{W}/\text{m}^2$  on the LED module at 2.5 W,  $T_a = 50^{\circ}\text{C}$  and at  $h = 10 \text{ W}/\text{m}^2\text{K}$

variation in the setup of model I except at the top portion (LED module). The temperatures of heat sink and cylindrical aluminium plate are minimum and they are in the value of permissible  $T_j$  values (less than  $125^{\circ}\text{C}$ ). The temperature distribution of top portion (LED module) is reached beyond its permissible limit and the magnified view of the same is mentioned in Fig. 8b. Fig. 8c shows the heat flux

Table 1.

Grid independence study of system without fin (model I) at 1.5 W

Elements ( $n$ )	Junction temperature, $T_j$ ( $^{\circ}\text{C}$ )				
	$T_a = 30^{\circ}\text{C}$	$T_a = 40^{\circ}\text{C}$	$T_a = 50^{\circ}\text{C}$	$T_a = 60^{\circ}\text{C}$	$T_a = 70^{\circ}\text{C}$
87500	94.45	104.45	114.75	124.65	134.71
112300	94.48	104.47	114.58	124.48	134.57
137000	94.49	104.48	114.53	124.42	134.52
162000	94.5	104.5	114.5	124.40	134.5
Error % between 112300 and 137000	0.0069	0.0191	0.026	0.0161	0.0149

in  $\text{W}/\text{m}^2$  on the LED module. Heat flux is almost uniform in the top of the LED module and it gradually increases towards the bottom of the LED module and thereafter the heat is diffused to the aluminium plate.

From this result, it is concluded that  $T_j$  values are in dangerous range, therefore, this analysis should be repeated for other  $T_a$  values and  $Q$  values. Simulations were run accordingly and the results are plotted in Fig. 9.

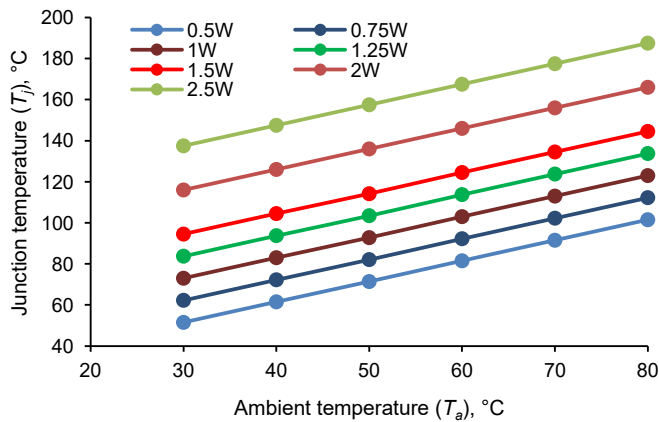


Fig. 9. Junction temperature ( $T_j$ ) variation with different ambient temperature ( $T_a$ ) and at different heat flow (at  $h = 10 \text{ W}/\text{m}^2\text{K}$ ) for model I

An analysis is carried out (for model I) to check the safety limit of LED lights when the heat flow and ambient temperature are varied. Simulations were carried out at different heat flow values and at different ambient temperatures ( $T_a$ ). Junction temperature ( $T_j$ ) values are estimated and it is shown in Fig. 9. It is found that the  $T_j$  varies linearly with  $T_a$  of LED light. It is noticed that for the heat flow of 1.25, 1.5, 2 and 2.5 W (most of the ambient temperatures),  $T_j$  is reached beyond its safety limit ( $125^{\circ}\text{C}$ ). Among the 42 operating conditions, 16 conditions failed to reach a comfortable  $T_j$  value. The failure percentage of operating conditions is 38%. If the safety limit goes beyond the critical value, there is a possibility of thermal risk.

Therefore, in such type of situations, the LED light needs fins or extended surfaces to diffuse the excess heat.

From Fig. 9, it is noticed that the ambient temperature ( $T_a$ ) varies linearly with junction temperature ( $T_j$ ). Therefore, a curve fitting procedure is performed and a correlation is developed in between the  $T_a$  and  $T_j$ . The developed correlation is,

$$T_j = mT_a + c, \quad (3)$$

where  $m$  is slope and  $c$  is constant and they are mentioned in Table 2.

Table 2.

Correlation constants and coefficients at  $h = 10 \text{ W/m}^2\text{K}$ ,  $D = 2 \text{ mm}$ ,  $L = 10 \text{ mm}$

Heat flow (W)	Slope $m$	Constant $c$	$R^2$
0.50	1.0003	21.461	1
0.75	1.0005	32.193	1
1.00	1.0007	42.923	1
1.25	1.0009	53.653	1
1.50	1.001	64.388	0.9999
2.0	1	85.99	1
2.5	1	107.49	1

From Table 2, it is noticed that the correlation coefficient ( $R^2$ ) for all the heat flow is 1. Therefore, it's a perfect fit and the correlation is correct. The slopes,  $m$  ( $dy/dx$ , is otherwise called as rise/run) of all the curves are also 1 (or approximately equal to 1). It means that for 1 unit  $T_j$  rise there is always 1 unit  $T_a$  run. By using this correlation, one can estimate  $T_j$ , if  $T_a$  value is known without further numerical simulations and it is applicable for model I. Since this slope is 1 (or approximately equal to 1), Eq. (3) can be written as,

$$T_j = T_a + c. \quad (4)$$

The results of model I show that the  $T_j$  values reached beyond its critical values for 16 conditions, therefore model II is developed with fins to check  $T_j$  values further. The results of model II are discussed in the next section.

### 3.2. Results of LED system with fin (model II)

Grid independence study was performed for model II, and  $T_j$  values were estimated at different  $T_a$  and at heat flow 1.5 W, fin diameter ( $D$ ) 2 mm, fin length ( $L$ ) 10 mm and  $h = 10 \text{ W/m}^2\text{K}$  and it is given in Table 3. The numbers of elements were chosen from 87500 to 162000. Table 3 shows the estimated  $T_j$  values at different  $T_a$  of 30°C, 40°C, 50°C, 60°C and 70°C for different number of elements ( $n$ ). At  $T_a = 30^\circ\text{C}$ , the average error between two junction temperatures

Table 3.

Grid independence study of system with fin (model II) at 1.5 W

Elements ( $n$ )	Junction temperature, $T_j$ ( $^{\circ}\text{C}$ )				
	$T_a = 30^{\circ}\text{C}$	$T_a = 40^{\circ}\text{C}$	$T_a = 50^{\circ}\text{C}$	$T_a = 60^{\circ}\text{C}$	$T_a = 70^{\circ}\text{C}$
97500	82.32	92.32	102.32	112.32	122.32
135000	82.42	92.43	102.4	112.39	122.4
185000	82.44	92.46	102.47	112.55	122.83
227000	82.45	92.47	102.48	112.56	122.84
Error % between 185000 and 227000	0.00325	0.0061	0.00884	0.00976	0.011

of successive elements of 185000 and 227000 was 0.00325%. Therefore, element ( $n$ ) 185000 was selected for this analysis.

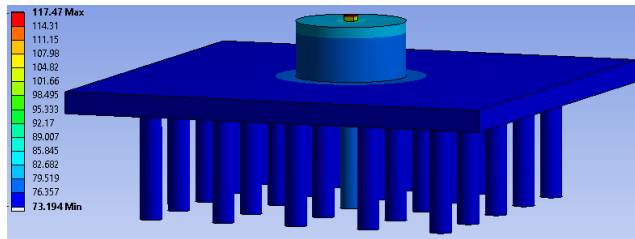
Fig. 10a shows the temperature distribution of model II in  $^{\circ}\text{C}$ . It is drawn at  $Q = 2.5\text{ W}$ ,  $T_a = 30^{\circ}\text{C}$  and  $h = 10\text{ W/m}^2\text{K}$ . Here too, as in Fig. 10a, the top portion of model II (LED module) had the temperature variation and in other locations, temperature was almost uniform. Also, it is noticed that the maximum temperature,  $T_j$  is  $117.47^{\circ}\text{C}$  which is within the permissible limit ( $125^{\circ}\text{C}$ ). Therefore, this operating condition ( $Q = 2.5\text{ W}$ ,  $T_a = 30^{\circ}\text{C}$  and  $h = 10\text{ W/m}^2\text{K}$ ) is safer for LED light. Fig. 10b shows the magnified view of top portion of model II (LED module). The top portion of LED module has higher temperature ( $117.47^{\circ}\text{C}$ ) and when the height is decreased from top to bottom, the temperature is decreased and it is in the range of  $92\text{--}101^{\circ}\text{C}$ . At the bottom of LED module, the heat is conducted to the aluminium plate and therefore, the temperature further decreases.

Fig. 10c shows the heat flux distribution in the LED module. Heat flux is increased from the top of the LED module to bottom. The maximum heat flux is observed at the bottom, especially at the bottom edges and corners. The heat transfer takes place from top to bottom, and when it reaches the bottom, the exposed area is reduced, especially at bottom edges and corners. Therefore, the heat flux is increased in those particular regions.

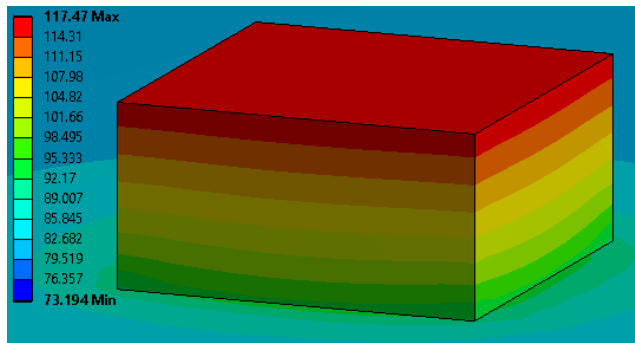
Heat flow is given to only top portion (LED module) and heat transfer takes place from LED module to the tip of the fin through conduction only. Since fins are used, heat loss continues through convection also.

This analysis should be done beyond the operating conditions ( $Q = 2.5\text{ W}$  and  $T_a = 30^{\circ}\text{C}$ ) to find other safer working conditions. Therefore, further simulations were run for different  $T_a$  values ( $30^{\circ}\text{C}$  to  $80^{\circ}\text{C}$ ) and at different  $Q$  values ( $0.5$  to  $2.5\text{ W}$ ) and the results are plotted in Fig. 11.

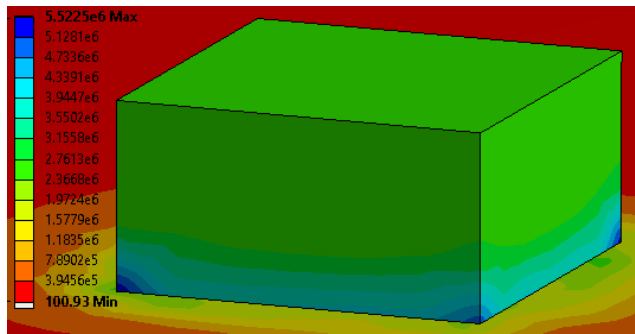
Simulations were carried out for model II and  $T_j$  values were estimated at different  $T_a$  and at different  $Q$  values, as shown in Fig. 11. The nature of results is the same as explained in Fig. 9.  $T_j$  is linearly varying with  $T_a$  (Fig. 11). Therefore, it is proved that  $T_a$  is an important factor while designing LED automobile lights. Also, it is noticed that  $T_j$  increases while heat flow is increased because of heat



(a)



(b)



(c)

Fig. 10. (a) Temperature distribution of model II in °C (a complete view), (b) Temperature distribution of top portion of model II (LED module) in °C, and (c) heat flux in  $W/m^2$  on the LED module at 2.5 W,  $T_a = 30^\circ C$  and at  $h = 10 W/m^2 K$

transfer through conduction. Here, the fin effect influenced  $T_j$  values and in most of the cases,  $T_j$  values are within permissible limits. The heat flow ( $Q$ ) values from 0.5 to 1.5 W and for all  $T_a$  values, and  $T_j$  values are in comfortable ranges as the fins are used to increase the heat transfer from LED light to outside air. If  $Q$  increases further (for 2 and 2.5 W) and for  $T_a$  values of 60, 70 and  $80^\circ C$ ,  $T_j$  values increase beyond the safety limit.

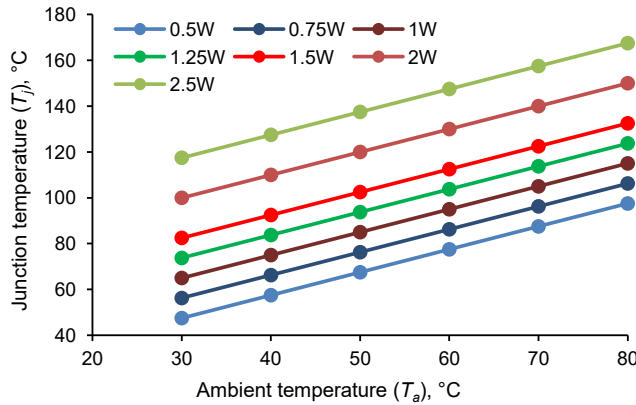


Fig. 11. Junction temperature ( $T_j$ ) variation with different ambient temperature ( $T_a$ ) and at different heat flow (at  $h = 10 \text{ W/m}^2\text{K}$ , fin diameter,  $D = 2 \text{ mm}$ , length,  $L = 10 \text{ mm}$ ) for model II

Therefore, it is concluded that model II gives comfortable  $T_j$  values for 33 operating conditions among 42 and 7 failed to reach the comfortable condition. The percentage of failure is reduced to 21.4% which is lower than model I's failure percentage (38%). It is proved that, for model II, the  $T_a$  range of 30 to 80°C and  $Q$  range of 0.5 to 1.25 W are safer range for LED lights as the safety limit is not crossed. Also, it can be noticed from Fig. 11 that lower  $T_a$  range from 30 to 40°C and all  $Q$  range from 0.5 to 2.5 W, is the safe range for LED lights as the safety limit is not crossed.

A curve fitting procedure was followed to develop a correlation between  $T_j$  and  $T_a$  for model II as they vary linearly. The developed correlation is,

$$T_j = mT_a + c, \quad (5)$$

where  $m$  is slope and  $c$  is constant and both are estimated by a regression analysis and mentioned in Table 4.

An analytical solution of fins was considered for estimating the heat transferred by the fins for the constant  $h$  of  $10 \text{ W/m}^2\text{K}$ , base temperature of fin,  $T_b = 125^\circ\text{C}$ ,

Table 4.

Correlation constants and coefficients at  $h = 10 \text{ W/m}^2\text{K}$ ,  $D = 2 \text{ mm}$ ,  $L = 10 \text{ mm}$

Heat flow (W)	Slope $m$	Constant $c$	$R^2$
0.50	1	17.494	1
0.75	1	26.241	1
1.00	1	34.988	1
1.25	1.0001	43.732	1
1.50	0.9999	52.485	0.9999
2.0	1	69.977	1
2.5	1	87.47	1



the ambient temperature ( $T_a$ ) was taken from 30 to 80°C. The heat transfer by the 25 fins was estimated as 1.55, 1.392, 1.23, 1.064, 0.9 and 0.736 W at different  $T_a$  of 30, 40, 50, 60, 70 and 80°C.

### 3.3. Effect of heat transfer coefficient on junction temperature ( $T_j$ )

LED light is placed in the automobile in a closed location to avoid water leakage during rain and to avoid interaction with moisture during high humidity. Though it is fitted in an air-tight enclosure, there may be a chance of air interaction inside the LED light enclosure because of the vehicle's fast movement and from inside air gaps. Therefore, there is a chance of air velocity inside and it can be approximated to being 0.1 to 0.5 m/s. It can be considered as natural convection [22] as these velocities are very small. During these velocity variations inside the domain, the heat transfer coefficient ( $h$ ) may also vary from 5 to 25 W/m<sup>2</sup>K [23] as  $h$  is a strong function of air velocity. Therefore, an analysis is carried out to estimate the junction temperature at different  $h$  values against the assumed values of 10 W/m<sup>2</sup>K in the previous chapter. For this analysis, a low temperature  $T_a$  is picked (40°C). The simulations were carried out at different  $h$  values (from 5 to 25 W/m<sup>2</sup>K) and the results are shown in Table 5. It is seen that the junction temperature is decreased when the  $h$  is increased. The heat transfer coefficient,  $h$  increases which implies that the convection heat transfer increases and hence the LED light loses its heat to the air. Therefore,  $T_j$  is decreased while  $h$  is increased and the same case was noticed for all  $Q$  values (Table 5). Also, it is noticed that at  $Q = 2.5$  W,  $T_j$  reached its highest value of 172.42°C at  $h = 5$  W/m<sup>2</sup>K, but when the  $h$  increases  $T_j$  reached its comfortable condition (less than 125°C).

Table 5.

Junction temperature ( $T_j$ ) at different  $h$  values and at different heat flow values at ambient temperature,  $T_a = 40^\circ\text{C}$

Heat transfer coefficient, W/m <sup>2</sup> K	Junction temperature ( $T_j$ ), °C						
	0.5 W	0.75W	1 W	1.25 W	1.5 W	2 W	2.5 W
5	66.49	79.7	92.9	106.2	119.45	145.94	172.42
10	57.5	66.3	74.8	83.7	92.48	109.98	127.47
15	54.5	61.7	68.9	76.2	83.48	97.98	112.47
20	52.9	59.5	65.6	72.5	78.79	91.96	104.95
25	52.1	58.1	64.2	70.2	76.26	88.35	100.43

### 3.4. Comparison of estimated junction temperature ( $T_j$ ) for both models

The estimated  $T_j$  values at different  $Q$  values and at different  $T_a$  values are compared for both models, model I and model II and mentioned in Table 6. Table 6 provides an opportunity to compare  $T_j$  values in adjacent column. For all the cases,

model II's  $T_j$  values are lower than model I. It is noticed that model II gives percentage of  $T_j$  reduction from the minimum value of 3.94% to the maximum value of 15.7%.

Table 6.  
Comparison of junction temperature ( $T_j$ ) at different ambient temperature ( $T_a$ ) for model I and model II

Heat flow (W)	Junction temperature, $T_j$ ( $^{\circ}\text{C}$ )					
	$T_a = 40^{\circ}\text{C}$		$T_a = 60^{\circ}\text{C}$		$T_a = 80^{\circ}\text{C}$	
	Model I	Model II	Model I	Model II	Model I	Model II
0.50	61.5	57.5	81.5	77.5	101.5	97.5
0.75	72.25	66.2	92.5	86.2	112.2	106.2
1.00	82.9	74.9	103	94.9	123	115
1.25	93.7	83.7	113.7	103.7	133.7	123.7
1.50	104.5	92.5	124.5	112.5	144.5	132.5
2	126	110	145.9	129.9	166	150
2.5	147.5	127.5	167.5	147.5	187.5	167.5

### 3.5. Model validation

The estimated  $T_j$  values at different ambient temperature and for model II (fin diameter,  $D = 2$  mm, fin length,  $L = 10$  mm,  $Q = 1.25$  W) are compared with the experimental results from X.-J. Zhao et al. [2] and shown in Fig. 12. The experimental solution [2]'s fin diameter is 2 mm and length is 17 mm. The minimum

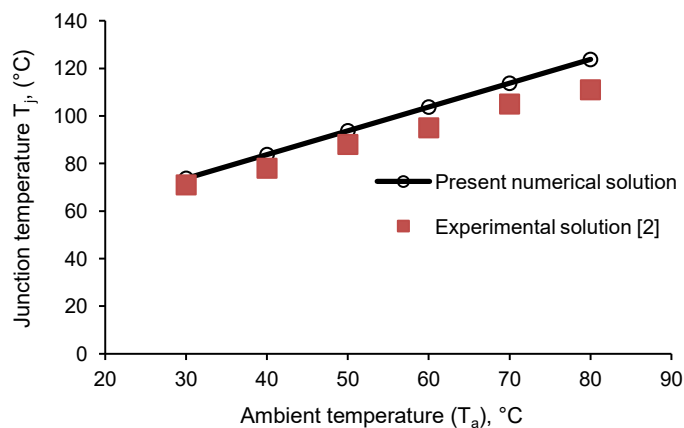


Fig. 12. Comparison of present results with experimental results from literature [2]

and maximum percentage errors of  $T_j$  are noticed as 3.8% and 11.5%, respectively. The error is maximum at  $T_a$  of 80°C and other values match those of the results obtained experimentally.

#### 4. Conclusions

A numerical method is developed to identify safer working conditions of an automobile LED light. There are two geometric models (LED light without fin – model I, with fin – model II) were generated using ANSYS Design Modeler and meshes were generated using ANSYS Multiphysics. Grid independence study was carried out to find the optimum number of grids. Two important working factors (ambient temperature and heat flow of LED bulbs) were considered as input parameters for this analysis to estimate the maximum temperature (junction temperature,  $T_j$ ) the LED light encounters while it works. The estimated  $T_j$  values of model II at  $Q = 1.25$  W was compared with experimental results from literature and it was found that the values were matching. The following conclusions were drawn:

- Initially the simulations were run with operating conditions of  $Q = 2.5$  W,  $T_a = 50^\circ\text{C}$  and  $h = 10$  W/m<sup>2</sup>K for model I (system without fin). It was concluded that the temperature distribution was almost uniform in all locations and also in a comfortable  $T_j$  range, but at the top of the setup (in LED module)  $T_j$  went beyond the safety limit.
- Further steps were taken to check the remaining operating conditions; therefore,  $T_a$  and  $Q$  were varied and the results were plotted. It was concluded that, among the 42 operating conditions, 16 conditions failed to reach the comfortable  $T_j$  values in model I.
- Simulations were run for model II (with fins) with the same operating conditions and it was concluded that the number of failures reduced from 16 to 9 in model II.
- Temperature variations of model I and model II were almost the same, but the maximum temperature ranges reduced from 187.5 to 167.5°C.
- Heat flux was estimated in the entire setup for both models (model I and model II) and found to have similar variations in both cases, as it was increased from top of the LED module and reached a maximum at bottom edges and corners because of the contraction of the exposed area.
- It is concluded that  $T_a$  ranges between 30 and 80°C and  $Q$  range of 0.5 to 1.25 W of model II is safer for LED automobile lights. Also, in the lower temperature range of  $T_a$ , of 30 to 40°C and for all  $Q$  values considered in this work (0.5 to 2.5 W) are safer operating conditions than any other conditions.
- A new correlation was developed between  $T_j$  and  $T_a$  for both models; therefore any one temperature can be found with the known value of other temperature without the necessity of further numerical simulations.
- Model II provided percentage reduction of  $T_j$  with a minimum of 3.94 to a maximum of 15.7% compared to model I.

## Acknowledgements

The author acknowledges with thanks the support received by way of proof reading from Dr. M.R. Vishwanathan, Assistant Professor of English, Humanities and Social Science Department, NIT Warangal, India.

Manuscript received by Editorial Board, April 13, 2019;  
final version, June 24, 2019.

## References

- [1] B.P. Minaker and Z. Yao. Design and analysis of an interconnected suspension for a small off-road vehicle. *Archive of Mechanical Engineering*, 64(1):5–21, 2017. doi: [10.1515/meceng-2017-0001](https://doi.org/10.1515/meceng-2017-0001).
- [2] X-J. Zhao, Y-X. Cai, J. Wang, X-H. Li, and C. Zhang. Thermal model design and analysis of the high-power LED automotive headlight cooling device. *Applied Thermal Engineering*, 75:248–258, 2015. doi: [10.1016/j.applthermaleng.2014.09.066](https://doi.org/10.1016/j.applthermaleng.2014.09.066).
- [3] D. Jang, S.J. Park, S.J. Yook, and K.S. Lee. The orientation effect for cylindrical heat sinks with applications to LED light bulbs. *International Journal of Heat and Mass Transfer*, 71:496–502, 2014. doi: [10.1016/j.ijheatmasstransfer.2013.12.037](https://doi.org/10.1016/j.ijheatmasstransfer.2013.12.037).
- [4] N. Wang, J. Liu, Q. Zhang, H. Yang, and M. Tan. Fatigue life evaluation and failure analysis of light beam direction adjusting mechanism of an automobile headlight exposed to random loading. *Proceedings of the Institution of Mechanical Engineers, Part D: Journal of Automobile Engineering*, 233(2):224–231, 2017. doi: [10.1177/0954407017740445](https://doi.org/10.1177/0954407017740445).
- [5] L. Sun, J. Zhu, and H. Wong. Simulation and evaluation of the peak temperature in LED light bulb heat sink. *Microelectronics Reliability*, 61:140–144, 2016. doi: [10.1016/j.microrel.2015.12.023](https://doi.org/10.1016/j.microrel.2015.12.023).
- [6] D. Luo, P. Ge, D. Liu, and H. Wang. A combined lens design for an LED low-beam motorcycle headlight. *Lighting Research & Technology*, 50(3):456–466, 2017. doi: [10.1177/1477153517697370](https://doi.org/10.1177/1477153517697370).
- [7] L. Kim, J.H. Choi, S.H. Jang, and M.W. Shin. Thermal analysis of LED array system with heat pipe. *Thermochimica Acta*, 455(1-2):21–25, 2007. doi: [10.1016/j.tca.2006.11.031](https://doi.org/10.1016/j.tca.2006.11.031).
- [8] X.-Y. Lu, T.-C. Hua, and Y.-P. Wang. Thermal analysis of high power LED package with heat pipe heat sink. *Microelectronics Journal*, 42(11):1257–1262, 2011. doi: [10.1016/j.mejo.2011.08.009](https://doi.org/10.1016/j.mejo.2011.08.009).
- [9] C.-S. Kim, J.-G. Lee, J.-H. Cho, D.-Y. Kim, and T.-B. Seo. Experimental study of humidity control methods in a light-emitting diode (LED) lighting device. *Journal of Mechanical Science and Technology*, 29(6):2501–2508, 2015. doi: [10.1007/s12206-015-0546-7](https://doi.org/10.1007/s12206-015-0546-7).
- [10] X.-Y. Lu, T.-C. Hua, M.-J. Liu, and Y.-X. Cheng. Thermal analysis of loop heat pipe used for high-power LED. *Thermochimica Acta*, 493(1-2):25–29, 2009. doi: [10.1016/j.tca.2009.03.016](https://doi.org/10.1016/j.tca.2009.03.016).
- [11] M. Janicki, T. Torzewicz, A. Samson, T. Raszkowski, A. Napieralski. Experimental identification of LED compact thermal model element values. *Microelectronics Reliability*, 86:20–26, 2018. doi: [10.1016/j.microrel.2018.05.003](https://doi.org/10.1016/j.microrel.2018.05.003).
- [12] K.C. Yung, H. Liem, and H.S. Choy. Heat transfer analysis of a high-brightness LED array on PCB under different placement configurations. *International Communications in Heat and Mass Transfer*, 53:79–86, 2014. doi: [10.1016/j.icheatmasstransfer.2014.02.014](https://doi.org/10.1016/j.icheatmasstransfer.2014.02.014).
- [13] M.W. Shin, and S.H. Jang. Thermal analysis of high power LED packages under the alternating current operation. *Solid-State Electronics*, 68:48–50, 2012. doi: [10.1016/j.sse.2011.10.033](https://doi.org/10.1016/j.sse.2011.10.033).

- 
- [14] J. Zhou, J. Huang, Y. Wang, and Z. Zhou. Thermal distribution of multiple LED module. *Applied Thermal Engineering*, 93:122–130, 2016. doi: [10.1016/j.applthermaleng.2015.09.022](https://doi.org/10.1016/j.applthermaleng.2015.09.022).
- [15] K.-S. Yang, C.-H. Chung, C.-W. Tu, C.-C. Wong, T.-Y. Yang, and M.-T. Lee. Thermal spreading resistance characteristics of a high power light emitting diode module. *Applied Thermal Engineering*, 70(1):361–368, 2014. doi: [10.1016/j.applthermaleng.2014.05.028](https://doi.org/10.1016/j.applthermaleng.2014.05.028).
- [16] K.-Y. Liao and S.H. Tseng. A superior design for high power GaN-based light-emitting diode packages. *Solid-State Electronics*, 104:96–100, 2015. doi: [10.1016/j.sse.2014.11.008](https://doi.org/10.1016/j.sse.2014.11.008).
- [17] K.F. Sokmen, E. Pulat, N. Yamankaradeniz, and S. Coskun. Thermal computations of temperature distribution and bulb heat transfer in an automobile headlamp. *Heat and Mass Transfer*, 50(2):199–210, 2014. doi: [10.1007/s00231-013-1229-5](https://doi.org/10.1007/s00231-013-1229-5).
- [18] I. Kim, S. Cho, D. Jung, C.R. Lee, D. Kim, and B.J. Baek. Thermal analysis of high power LEDs on the MCPCB. *Journal of Mechanical Science and Technology*, 27(5):1493–1499, 2013. doi: [10.1007/s12206-013-0329-y](https://doi.org/10.1007/s12206-013-0329-y).
- [19] V.P. Chandramohan and P. Talukdar. Three dimensional numerical modeling of simultaneous heat and moisture transfer in a moist object subjected to convective drying. *International Journal of Heat Mass Transfer*, 53(21-22):4638–4650, 2010. doi: [10.1016/j.ijheatmasstransfer.2010.06.029](https://doi.org/10.1016/j.ijheatmasstransfer.2010.06.029).
- [20] S. Yadav, A.B. Lingayat, V.P. Chandramohan, and V.R.K. Raju. Numerical analysis on thermal energy storage device to improve the drying time of indirect type solar dryer. *Heat and Mass Transfer*, 54(12):3631–3646, 2018. doi: [10.1007/s00231-018-2390-7](https://doi.org/10.1007/s00231-018-2390-7).
- [21] G. Arunsandeep and V.P. Chandramohan. Numerical solution for temperature and moisture distribution of rectangular, cylindrical and spherical objects during drying. *Journal of Engineering Physics and Thermophysics*, 91(4):895–906, 2018. doi: [10.1007/s10891-018-1814-z](https://doi.org/10.1007/s10891-018-1814-z).
- [22] T.A. Alves, P.H.D. Santos, and M.A. Barbur. An invariant descriptor for conjugate forced convection-conduction cooling of 3D protruding heaters in channel flow. *Frontiers of Mechanical Engineering*, 10(3):263–276, 2015. doi: [10.1007/s11465-015-0345-y](https://doi.org/10.1007/s11465-015-0345-y).
- [23] T.L. Bergman, F.P. Incropera, D.P. Dewitt, and A.S. Lavine. *Fundamentals of Heat and Mass Transfer*. 7th edition. John Wiley & Sons, 2011.